Talanta 220 (2020) 121398

Contents lists available at ScienceDirect

Talanta

journal homepage: www.elsevier.com/locate/talanta

Sensitive biosensor for p53 DNA sequence based on the photothermal effect of gold nanoparticles and the signal amplification of locked nucleic acid functionalized DNA walkers using a thermometer as readout

Yingzhou Tao [a,1], Weijia Wang [b,1], Caili Fu [c], Fang Luo [a,c,**], Longhua Guo [a], Bin Qiu [a], Zhenyu Lin [a,*]

[a] MOE Key Laboratory for Analytical Science of Food Safety and Biology, Fujian Provincial Key Laboratory of Analysis and Detection Technology for Food Safety, College of Chemistry, Fuzhou University, Fuzhou, 350116, China
[b] Zhongshan People's Hospital, Zhongshan, Guangdong, 528403, China
[c] College of Biological Science and Engineering, Fuzhou University, Fuzhou, Fujian, 350116, China

ARTICLE INFO

Keywords:
Photothermal biosensor
Aggregated AuNPs
DNA walkers
Locked nucleic acid
Photothermal effect

ABSTRACT

A convenient photothermal biosensor was constructed for p53 DNA sequence detection based on the high discrimination capability of locked nucleic acid and high efficiency of signal amplification strategy of DNA walkers and difference photothermal effect between aggregated and dispersed gold nanoparticles (AuNPs). The presence of target activated the DNA walkers via the high affinity between target and complementary locked nucleic acid in the probe strand, resulting in the hybridization of the walker strand and substrate strand to form a specific enzyme recognition site. Under the cleavage of the endonuclease, single-stranded DNA (ssDNA) was released to the solution. Then the walker strand bound to a new substrate strand, and the next round of cleavage was triggered. The released ssDNA enhanced the stability of AuNPs against salt-induced aggregation. Given difference photothermal effects of the aggregated AuNPs and dispersed AuNPs under the near-infrared laser, the change of the temperature was detected by a common thermometer easily, which had a linear relationship with the target concentration in the range of 2.0–120.0 pM, the detection limit was 1.4 pM (S/N = 3). The proposed photothermal assay has been applied to detect p53 DNA sequence spiked complex samples with satisfying results.

1. Introduction

Cancer is a fatal disease on a global scale, killing millions of people every year and hence receiving much attention [1,2]. High post-operative survival rate can be achieved with early diagnosis and timely surgery. The p53 gene, a cancer suppressor gene, is associated with regulating cell cycle and cell metabolism [3,4]. Mutational p53 gene can cause the loss of normal function and triggers the growth and metastasis of cancer cells, and it can be found in human tumors frequently [5–9]. Therefore, it is significant to develop some sensitive and specific methods for the p53 gene detection in early cancer screening.

Many techniques, such as electrochemistry, fluorescence, chemiluminescence, and electrochemiluminescence, have been applied to quantify the p53 gene with high sensitivity [3,10–16]. However, most methods need bulk advanced analytical equipment and well-trained labor, limiting their applications in resource-limited areas. Point-of-care testing (POCT), possessing a variety of advantages such as low cost, small size, and easy operation, is promising to be used in resource-limited settings. Several POCT technologies have been constructed for p53 DNA sequence quantification. For instance, using a personal glucose meter as readout, a simple and affordable strategy has been designed for p53 DNA detection by integrating signal amplification strategy with invertase-catalyzed sucrose hydrolysis to generate glucose [17]. Yu's group has developed a colorimetric detection system for the p53 DNA sequence by using peroxidase-mimicking DNAzyme-mediated oxidation of substrates to generate color change which can be observed

* Corresponding author.
** Corresponding author. MOE Key Laboratory for Analytical Science of Food Safety and Biology, Fujian Provincial Key Laboratory of Analysis and Detection Technology for Food Safety, College of Chemistry, Fuzhou University, Fuzhou, 350116, China.
E-mail addresses: luofang@fzu.edu.cn (F. Luo), zylin@fzu.edu.cn (Z. Lin).
[1] These authors contribute equally to this work.

https://doi.org/10.1016/j.talanta.2020.121398
Received 15 May 2020; Received in revised form 2 July 2020; Accepted 8 July 2020
Available online 21 July 2020

by the naked eye [18]. These studies suggested that POCT for p53 DNA sequence detection is practical and simple. However, it is still necessary to explore new portable signal reading device for POCT of p53 DNA sequence.

Thermometer can be found nearly in every home, which possesses the inherent advantages of low cost, high accuracy, and easy operation. The application of thermometer has been expanded and applied as a readout device in the biosensors [19]. Most of the photothermal biosensors are designed according to nanoparticle-mediated photothermal effect and immunoassay [20–22]. The target trigger aggregation of gold nanoparticle (AuNPs) has been used in the development of colorimetric methods using nake eyes as readout frequently. Due to the high light absorption in the NIR area, aggregated AuNPs exhibit strong light-to-heat conversion. Recently, the photothermal effect of aggregated AuNPs has been used to develop analytical methods employing the thermometer as the signal readout device. For example, our group has developed a novel and simple aptamer-based photothermal biosensor for the detection of small molecule utilizing the photothermal effect of aggregated AuNPs. Target-mediated conformation change of aptamer would promote salt-induced AuNPs aggregation and hence enhances photothermal effect in the NIR area. Thus, the detection of target could be converted into a temperature measurement using a handheld thermometer [23]. Similarly, Li's group has reported a photothermal detection system using the strong light-to-heat conversion of aggregated AuNPs and DNA hybridization. DNA hybridization can alter the distance of AuNPs, resulting in an obvious change of photothermal effect which can be measured by a thermometer [24]. However, many efforts are still needed to apply the photothermal effect of aggregated AuNPs in the developing biosensor for broader targets.

The DNA walkers is a nuclease drive molecular machine which can move along designed tracks based on the Watson–Crick base pairing principle. Once activated by an initiator, the DNA walkers can repeat mechanical cycles and hence realizes the release of the substrate strand. The DNA walkers has the characters of predictable, rapidness, and extraordinary programmable and had been applied to develop biosensor for diverse targets [25–30]. Locked nucleic acid (LNA) has high ability to discriminate target sequence due to its unique conformation. The methylene bridge in LNA increases binding affinity for complementarity sequences and endows LNA with attractive selectivity [31]. These two techniques can be combined together to develop high sensitive and specific biosensors for different DNA sequences [32].

The presence of a large amount of single-stranded DNA (ssDNA) can adsorb on the surface of AuNPs and resists the salt-induced AuNPs aggregation. This character has been applied to develop colorimetric biosensors. Early study indicated that there is difference photothermal effect between the aggregated AuNPs and dispersed AuNPs. In this study, this property has been applied to develop a convenient photothermal biosensor for p53 DNA sequence, through the combination of LNA and DNA walkers. Once the target was introduced, it hybridized with the LNA-modified probe due to the strong affinity of the LNA toward complementary sequence, resulting in the activation of the DNA walkers. Subsequently, the activated DNA walkers would repeat the cycles of hybridization and cleavage, releasing a large amount of ssDNA to resist salt-induced aggregation of AuNPs. In this case, the light-to-heat conversion of the system could decrease. The detection for the p53 DNA sequence can be achieved by measuring the temperature change value of the system under laser irradiation using a thermometer as readout.

2. Experimental section

2.1. Materials and chemicals

Streptavidin magnesphere paramagnetic particle (PMPs) were acquired from Promega Corporation (Madison, USA). Chloroauric acid tetrahydrate ($HAuCl_4{\cdot}4H_2O$) and Sodium citrate were acquired from Sinopharm Chemical Reagent (Shanghai, China). Nicking endonuclease (Nb.BbvCI) was obtained by New England Biolabs (Beijing, China). SYBR Green II was acquired from Xiamen Biovision Biotechnology (Xiamen, China). Other reagents were of analytical grade and used directly without further purification. The ssDNA used herein was synthesized and purified by Sangon Biotech (Shanghai, China). The sequences of the involved oligonucleotides are listed below:

p53: 5'- TCA TCA CAC TGG AAG ACT C -3'.

Probe strand (P): 5'- TGA GGG AGT CTT CCA GTG TGA TGA -3' (*G* was modified by LNA).

Walker strand (W): 5'-biotin- TTT TTT TTT TTT TTT TTT TTT TTT TTT TTT TTT TTT TTT TTT TTT TGG AAG ACT CCC TCA G C -3.

Substrate strand (S): 5'-biotin-TTT TTT GCT GAG GTA CGA GGT TGT AT-3'.

Single-base mismatched DNA (T1): 5'- TCA TGA CAC TGG AAG ACT C-3'.

Double-base mismatched DNA (T2): 5'-TCA AGA CAC TGG AAG ACT C-3'.

Non-complementary DNA (Tn): 5'- GGT CTC TTG ATA GCA CTC A -3'.

2.2. Instruments

The TEM imaging was performed on a Tecnai G2 F20 STWIN microscope operating at 200 kV. UV–vis absorption spectra were measured using a Microplate spectrophotometer (Multiskan GO, Thermo Scientific, USA). The temperature measurement was performed on a digital thermometer (CIE305P; Purchased from Lianhong Electronic Instruments Co. LTD). A portable NIR laser (1.5 W, 750 nm) was used for irradiating the solution.

2.3. Synthesis of AuNPs

AuNPs were synthesized based on early literature [33,34]. Detailed methods can be found in our previous work [23].

2.4. Construction of DNA walkers

Firstly, biotin modified walker strand (W) and the LNA modified probe strand (P) were mixed in a Tris buffer solution (containing 10 mM $MgCl_2$, 50 mM NaCl, 10 mM Tris-HCl, pH 7.4) and hold for 5 min at 90 °C. The P hybridized with W by slowly being cooled to 37 °C to form PW. A portion of PMPs (100 μL 1 mg/mL) were washed by PBS buffer containing 0.02% Tween-20 three times and then dispersed in 27.5 μL PBS buffer. The PMPs were mixed with the substrate strand (S) and the PW in PBS buffer (total volume was 100 μL, containing 2 μM S and 200 nM PW). The mixture was hold for 2 h at 37 °C. Then, the supernatant (containing excess P) was removed by magnetic separation and the PMPs were dispersed in 100 μL of water for future use.

2.5. DNA walkers reaction

The modified PMPs (10 μL) were mixed with a buffer containing different concentrations of the target (total volume of the mixture was 19 μL, containing 10 mM Tris-HCl, 10 mM $MgCl_2$, 50 mM NaCl, pH 7.4). The reaction was incubated at 37 °C for 15 min. Then, the PMPs were collected by magnetic separation and dispersed in 20 μL Nb.BbvCI enzyme solution (containing 5 U of Nb.BbvCI enzyme, 10 mM Tris-HCl, 10 mM $MgCl_2$, 50 mM NaCl, pH 7.4). After the reaction at 37 °C for 10 min, the supernatant of the mixed solution was collected for later use.

2.6. Gel electrophoresis and fluorescence measurement

Polyacrylamide gel electrophoresis (12%, PAGE) and fluorescence were used to confirm the products of the DNA walkers. Before the fluorescence analysis, the sample was incubated with SYBR Green II (which can combine with ssDNA to produce fluorescence signals) under

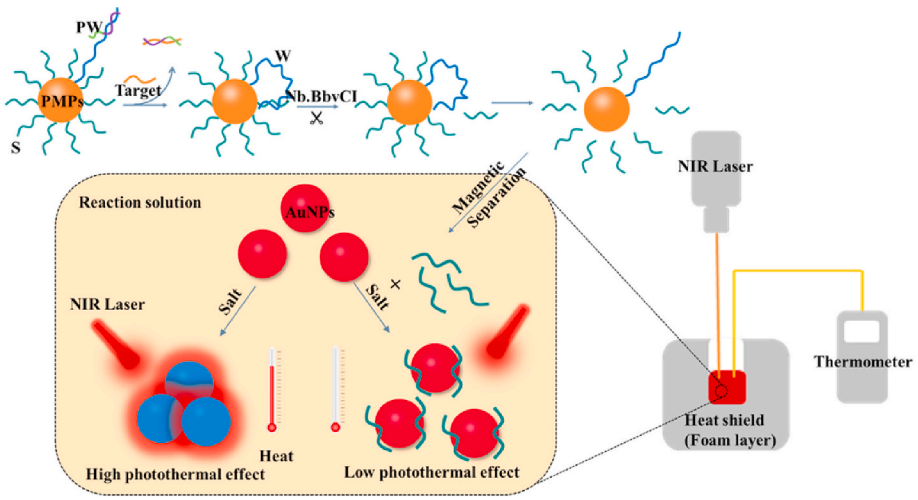

Scheme 1. Schematic mechanism of the photothermal biosensor based on DNA walkers for the detection of p53 DNA sequence.

37 °C for 15 min. The excitation wavelength used in the fluorescence analysis was 480 nm.

2.7. Photothermal assay of p53 DNA sequence

The DNA walkers product was mixed with NaCl solution firstly. The total volume of the mixed solution was 50 μL, and the concentration of NaCl was 100 mM. Subsequently, the AuNPs (200 μL) was introduced. The temperature change of the mixed solution was monitored by a digital thermometer. To reduce the heat exchange between the reaction solution and the environment, a foam layer was used as a heat shield around the reaction solution in all experiments. The room temperature was kept at 26 °C.

2.8. Photothermal assay in human serum

Firstly, proteinase K (400 μg/mL) was used for the preincubation of human serum samples (from volunteers) at 37 °C for 1 h. Then, the treated human serum was diluted with 1 × NEBuffer 3. Subsequently, p53 DNA sequence were introduced in diluted human serum (10%) and detected according to the above procedure.

3. Results and discussion

3.1. Design of the DNA walkers based photothermal assay

Scheme 1 shows the mechanism of the photothermal assay for the p53 DNA sequence. This photothermal detection system consists of four parts: Laser; Reaction solution; Heat shield; Thermometer. A NIR laser was used as the light source to irradiate the reaction solution. The reaction solution was comprised of the AuNPs and different DNA walker products. The heat shield was a foam layer around the reaction solution to reduce the heat exchange between the reaction solution and the environment. The digital thermometer was used to record the temperature change. S and W are modified on the surface of PMPs via biotin-streptavidin conjugation. The end of the S has a recognition sequence 5′-GC*TGAGG-3’ (where * is the cleavage site), which can be activated only when it forms a double strand with the complementary strand. The W is firstly hybridized with a moiety of LNA-modified P to form PW to lock the cleavage site. In the present of p53 gene, the LNA-modified P would bind to the p53 gene through the strong hybridization affinity with high discrimination. After the hybridization between p53 gene and P, the end of W would be exposed and hybridized with the bottom

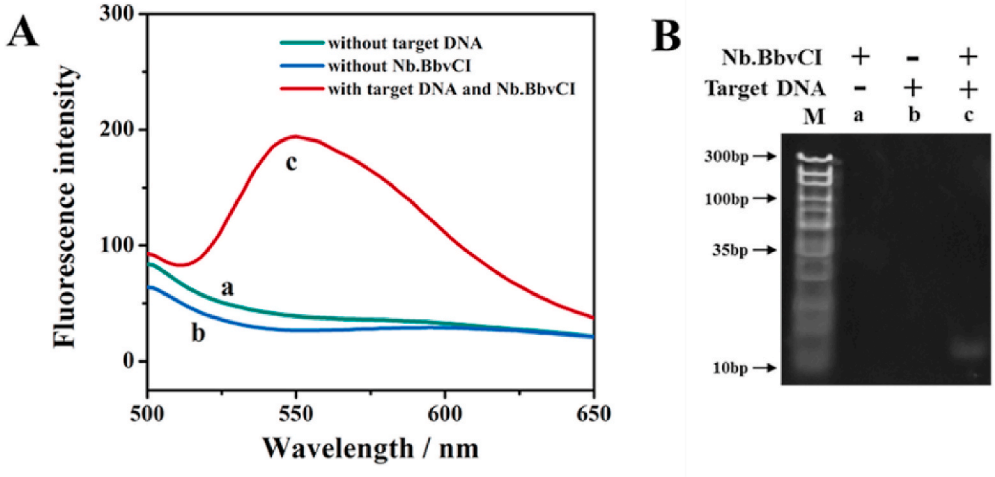

Fig. 1. (A) The fluorescence analysis of the DNA walkers products: (a) without the target DNA, (b) without Nb.BbvCI, and (c) with target DNA and Nb.BbvCI. (B) PAGE analysis of the DNA walkers products. The experimental conditions for lanes a–c were indicated above; Lane M: DNA size marker. 120 pM target DNA, 5.0 U of Nb.BbvCI were used in the assay.

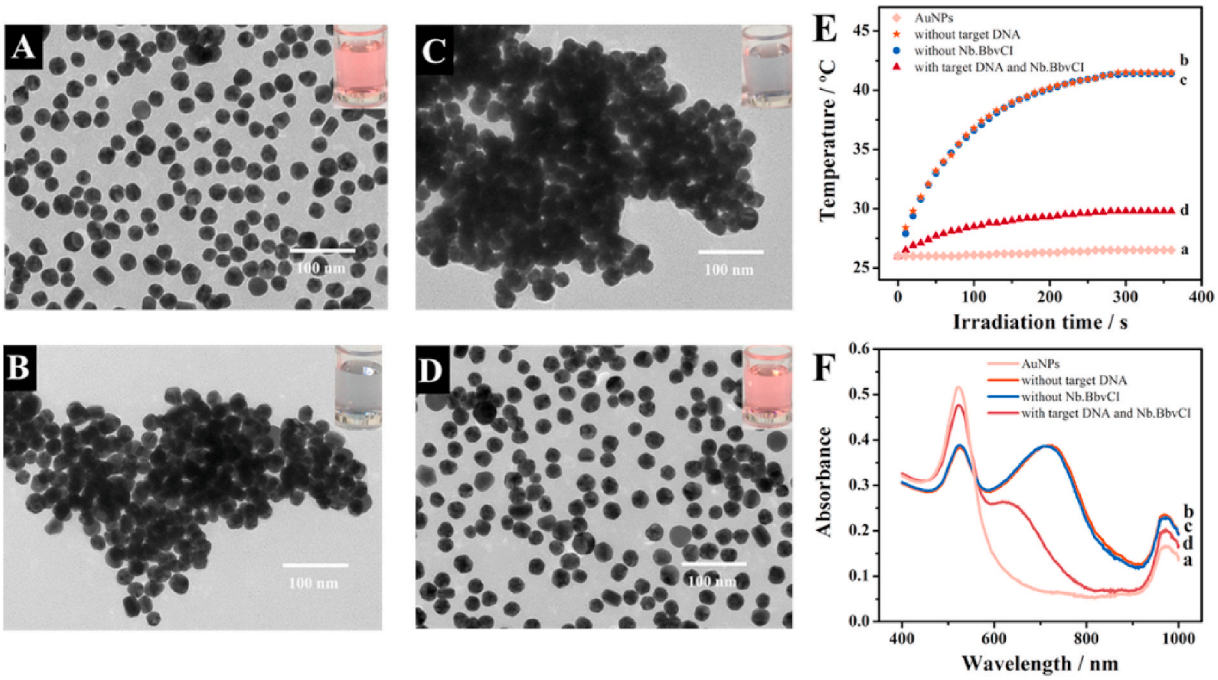

Fig. 2. Typical TEM images of AuNPs under different conditions (A) original AuNPs, (B–D) AuNPs mixed with different DNA walkers products; (B)without the target DNA; (C)without the Nb.BbvCI; (D)with target DNA and Nb.BbvCI. (Insets: photographs of the corresponding samples); (E) Temperature comparison and (F) UV–vis absorption spectra of AuNPs under different conditions (a) original AuNPs, (b–d) AuNPs mixed with different DNA walkers products– (b) without the target DNA, (c) without the Nb.BbvCI, and (d) with target DNA and Nb.BbvCI. 200 μL AuNPs, 120 pM target DNA, 5.0 U of Nb.BbvCI were used in the assay.

regions of the S, which is able to activate the cleavage site. At this time, the Nb.BbvCI enzyme specifically cleaves the recognition sequence, resulting in the release of S from PMPs. The W continues to hybridize with the next S and therefore triggers the next circulation of cleavage, which results in a larger amount of ssDNA were released in the solution. By magnetic separation, the PMPs with the uncleaved ssDNA is removed. The released ssDNA in the supernatant can help the AuNPs to be evenly dispersed at high salt concentration. When the p53 DNA sequence is absent, the enzymatic cleavage reaction cannot be triggered, in this case, there is no ssDNA in the supernatant and hence the AuNPs would be aggregated under high salt concentration. The principle of this study lies in that the aggregated and dispersed AuNPs have different photothermal effect under NIR laser, because aggregated AuNPs can effectively absorb NIR light while the other AuNPs has week absorption in NIR region. The different photothermal effect between the aggregated and dispersed AuNPs can be measured by a thermometer easily. The presence of target can produce a lot of ssDNA during signal amplification of DNA walking, which can prevent the aggregation of AuNPs. And the degree of the aggregation has some relationship with the amount of ssDNA. Based on these properties, a convenient and sensitive photothermal assay method was developed for p53 gene detection through the target-induced aggregated/dispersed state change of AuNPs.

3.2. *Feasibility of the DNA walkers based photothermal assay*

The production of large amounts of ssDNA is a key factor in the designing of the experiments, which can be characterized by fluorescence and gel electrophoresis assay easily. SYBR Green II, which can combine with ssDNA to produce fluorescence signals, was used to check whether the products of the DNA walkers contain ssDNA. As obtained in Fig. 1A, no significant signal was presented when the p53 DNA sequence (curve a) or Nb.BbvCI (curve b) was absent, while a significant fluorescence signal can be detected when the p53 DNA sequence was introduced (curve c). These results confirmed that p53 DNA sequence could initiate the DNA walkers reaction. The result of the gel electrophoresis assay was shown in Fig. 1B. In the absence of the p53 DNA sequence (lane a) or Nb.BbvCI (lane b), no obvious electrophoresis bands were observed. When the p53 DNA sequence and the Nb.BbvCI enzyme were both present (lane c), a band (bottom) was observed, demonstrating the production of a large amount of ssDNA.

Then, TEM images were used to confirm the change of AuNPs states. As shown in Fig. 2A, the synthesized AuNPs were uniformly dispersed. However, when the AuNPs were mixed with DNA walkers products without p53 DNA sequence under a high salt concentration, and the AuNPs were aggregated (Fig. 2B). Similarly, as shown in Fig. 2C, when the AuNPs were mixed with DNA walkers products without Nb.BbvCI, the aggregation of AuNPs were observed. Fig. 2D is AuNPs mixed with DNA walkers products with both p53 DNA sequence and Nb.BbvCI. Under the high salt concentration, the AuNPs were uniformly dispersed. These results indicated that the products of the DNA walkers could enable the AuNPs to be uniformly dispersed under salt solution.

As shown in Fig. 2E, under laser illumination, the temperature of the synthesized AuNPs changed slowly in 6 min (curve a). However, when the p53 DNA sequence (curve b) or Nb.BbvCI (curve c) was absent, the mixture of AuNPs and DNA walkers products had an obvious temperature increase. With the addition of the p53 DNA sequence and Nb.BbvCI (curve d), the temperature of the mixed solution of AuNPs and DNA walkers products raised slowly under illumination, which is similar to that of the synthesized AuNPs, indicating that AuNPs are protected by ssDNA. These results demonstrate the feasibility of the principle for p53 DNA sequence detection.

The UV–vis absorption spectrum was measured for the further study of mechanism. As demonstrated in Fig. 2F, the prepared AuNPs had an absorption peak at ~520 nm, and the absorption value in the NIR region was weak (curve a). When the p53 DNA sequence (curve b) or Nb.BbvCI (curve c) was absent, the absorption peak of the mixed solution of AuNPs and DNA walkers products was shifted to the NIR region. The shifting of plasmon resonance wavelength is probably caused by the distance-dependent optical properties of the AuNPs. As shown in curve d, upon the addition of p53 DNA sequence and Nb.BbvCI to the DNA walkers, the AuNPs mixed solution had a UV–vis absorption peak similar to that of the uniformly dispersed AuNPs, indicating that the ssDNA released from

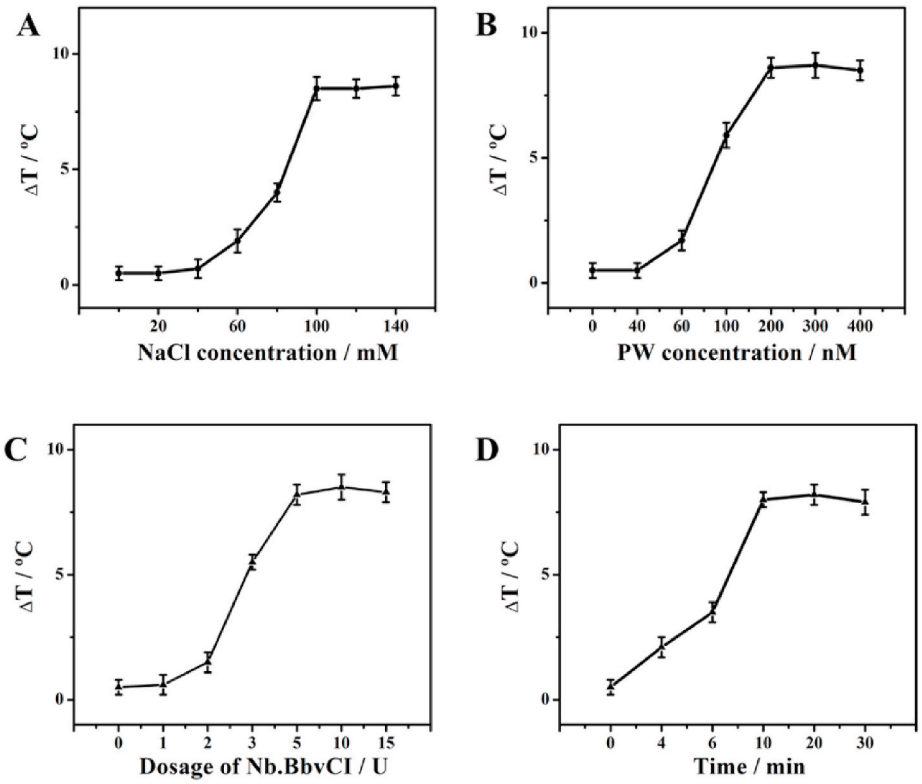

Fig. 3. Optimization of experimental conditions (A) Effect of the concentration of NaCl, (B) Effect of the concentration of PWs, (C) Effect of the concentration of Nb.BbvCI, (D) Effect of the digestion time of Nb.BbvCI. 80 pM target DNA was used in the assay. Error bars are standard deviations of three repetitive experiments.

DNA walkers can improve the stability of the AuNPs.

3.3. Optimization of the reaction conditions

The effect of NaCl concentration, PW concentration, Nb.BbvCI concentration, digestion time of Nb.BbvCI on the performance for p53 DNA sequence detection were tested. The NaCl concentration was first optimized because this governed the aggregation of AuNPs. As shown in Fig. 3A, the temperature change (ΔT, the difference temperature increase between the absence and presence of target) increased with the increment of salt concentration and remained approximately constant after 100 mM. Therefore, 100 mM of NaCl was selected for further assays. Subsequently, the influence of the amount of PW was tested. Fig. 3B shows that ΔT increased as the amount of PW increased. When the concentration of the PW was higher than 200 nM, ΔT remained approximately constant, indicating that the concentration of the PW is sufficient to trigger the DNA walkers. Therefore, 200 nM of PW was chosen for the next study.

The amount of Nb.BbvCI and the time of the digestion of Nb.BbvCI can affect the concentration of the ssDNA cleaved, thus affecting the dispersion state of the AuNPs. So the amount of enzyme and the digestion time were optimized. Fig. 3C shows that the temperature change value increased as the amount of enzyme increased, but when the amount of enzyme reached 5.0 U, the temperature change value did not change significantly. As shown in Fig. 3D, when the digestion time was more than 10 min, the temperature change value did not rise any more. Therefore, the amount of enzyme used was 5.0 U and the digestion time was 10 min.

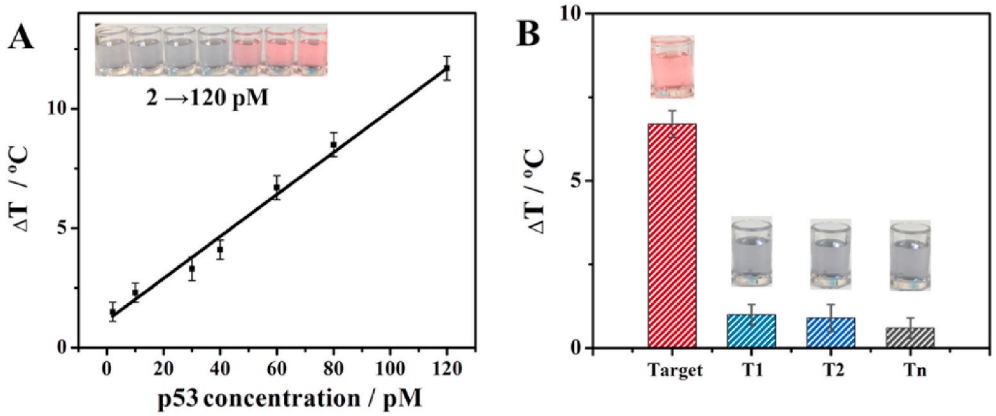

Fig. 4. (A) The relationship between ΔT and the p53 gene concentration; (B) The selectivity of the proposed photothermal assay towards the p53 gene. (Insets: photographs of the corresponding samples).

Table 1
Recovery test of p53 DNA sequence spiked in human serum using the proposed photothermal biosensor (n = 3).

Sample	Target DNA spiked (pM)	Target DNA detected (pM)	Recoveries (%)	RSD (%)
1	10.0	9.3	93.0	4.9
2	20.0	18.7	93.5	3.6
3	50.0	53.9	107.8	4.3

3.4. Analytical performance

The photothermal analysis of p53 DNA sequence was carried out under the optimum conditions. As presented in Fig. 4A, the ΔT measured by thermometer increased with the increasing target concentration. A good linear relationship was observed ranging from 2.0 to 120.0 pM ($\Delta T = 0.088\ C_{[p53]} + 1.085$, $R^2 = 0.986$) and the detection limit (LOD) was 1.4 pM (S/N = 3). The significant color changes caused by the aggregation of AuNPs were usually allowing designs of the colorimetric platform. Therefore, the sensitivity of the colorimetric assay for p53 DNA sequence was studied as well. Inset in Fig. 4A is the photographs of corresponding AuNPs samples. As shown in the inset, with the decrease of p53 DNA sequence concentration, a red-to-blue color change was presented. The LOD for the p53 DNA sequence was 60 pM by naked eyes, which is higher than that obtained by the thermometer. Moreover, benefiting from the signal amplification of the DNA walkers, the sensitivity of the proposed biosensor for p53 DNA sequence is even higher than that reported in previous papers without the use of bulk instrument [35–38].

To test the selectivity of the photothermal biosensor, non-complementary DNA (Tn), single-base mismatched DNA (T1), and two-base mismatched DNA (T2) were used in a control assay. The concentration of Tn, T1, and T2 was set as 10 times (600 pM) as that of p53 DNA sequence (60 pM). As presented in Fig. 4B, the ΔT had a significant change only when the p53 DNA sequence was added. Insets in Fig. 4B are the photograms of the corresponding AuNPs samples. In the presence of p53 DNA sequence, the color of AuNPs remains unchanged. However, a significant red-to-blue color change was observed in the presence of T1, T2, or Tn. This color change is consistent with the ΔT change, indicating that only the introduction of the p53 DNA sequence can activate the DNA walkers to protect the AuNPs from aggregation. These results demonstrated that the designed photothermal biosensor has great selectivity for p53 DNA sequence, probably because the LNA modified DNA walkers has a high discrimination capability.

3.5. Analytical application in real samples

To further test the capability of the photothermal biosensor in complex samples, p53 DNA sequence spiked in diluted human serum (10%) was measured. As shown in Table 1, the recovery rates were varied in 93.0–107.8%, and the relative standard deviations (RSDs) were lower than 5.0%. These results imply that it is possible to use this photothermal biosensor in complex samples.

4. Conclusion

In summary, a convenient photothermal biosensor with high sensitivity and selectivity has been explored for the detection of the p53 DNA sequence with the assistance of the photothermal effect of the aggregated AuNPs and locked nucleic acid functionalized DNA walkers. By coupling the amplification efficiency of DNA walkers and the discrimination capability of LNA, the developed photothermal biosensor for the p53 DNA sequence has a low LOD of 1.4 pM and a linear range of 2.0–120.0 pM without advanced analytical instruments. Furthermore, with outstanding programmability of DNA walkers, the designed photothermal biosensor may be exploited to detect varied targets by modifying other DNA sequences. The hand-held NIR laser that we used as the light energy source is very cheap compared to the spectrometer, however, the price of laser is still relatively higher than a thermometer. The development of commercial lasers may future reduce the price of handheld lasers and the cost of photothermal analysis.

CRediT author statement

Yingzhou Tao: Conceptualization, Methodology, Investigation, Writing - Original Draft. Weijia Wang: Formal analysis, Validation. Caili Fu:Visualization. Fang Luo: Software, Project administration, Writing - Review & Editing. Longhua Guo: Formal analysis, Validation. Bin Qiu: Visualization. Zhenyu Lin: Resources, Review & Editing, Supervision.

Declaration of competing interest

The authors declare that they have no known competing financial interests or personal relationships that could have appeared to influence the work reported in this paper.

Acknowledgements

This project was financially supported by National Science Foundation of China (21904020, 21974020), the cooperative project of production and study in University of Fujian Province (2018Y4007), the Sciences Foundation of Fujian Province (2018J05018, 2018J01685, 2018J01682), “Thirteenth Five-Year Plan” Marine Economy Innovation and Development Demonstration Project (Grant No. FZHJ19).

References

[1] F. Bray, J. Ferlay, I. Soerjomataram, R.L. Siegel, L.A. Torre, A. Jemal, Global cancer statistics 2018: GLOBOCAN estimates of incidence and mortality worldwide for 36 cancers in 185 countries, CA-Cancer J. Clin. 68 (2018) 394–424.
[2] A. Nicolini, P. Ferrari, M.J. Duffy, Prognostic and predictive biomarkers in breast cancer: past, present and future, Semin. Canc. Biol. 52 (2018) 56–73.
[3] H. Dong, Z.-S. Wu, J. Xu, J. Ma, H. Zhang, J. Wang, W. Shen, J. Xie, L. Jia, Novel multifunction-integrated molecular beacon for the amplification detection of DNA hybridization based on primer/template-free isothermal polymerization, Biosens. Bioelectron. 72 (2015) 182–190.
[4] A.J. Levine, J. Momand, C.A. Finlay, The p53 tumour suppressor gene, Nature 351 (1991) 453–456.
[5] E.B. Aydin, M. Aydin, M.K. Sezginturk, Electrochemical immunosensor based on chitosan/conductive carbon black composite modified disposable ITO electrode: an analytical platform for p53 detection, Biosens. Bioelectron. 121 (2018) 80–89.
[6] L. Wang, M. Yao, X. Fang, X. Yao, Novel competitive chemiluminescence DNA assay based on Fe3O4@SiO2@Au-functionalized magnetic nanoparticles for sensitive detection of p53 tumor suppressor gene, Appl. Biochem. Biotechnol. 187 (2019) 152–162.
[7] B. Vogelstein, D. Lane, A.J. Levine, Surfing the p53 network, Nature 408 (2000) 307.
[8] K.H. Vousden, X. Lu, Live or let die: the cell’s response to p53, Nat. Rev. Canc. 2 (2002) 594.
[9] M. Olivier, M. Hollstein, P. Hainaut, TP53 mutations in human cancers: origins, consequences, and clinical use, Csh. Perspect. Biol. 2 (2010) a001008.
[10] H. Wei, Y. Du, J. Kang, E. Wang, Label free electrochemiluminescence protocol for sensitive DNA detection with a tris(2,2′-bipyridyl)ruthenium(II) modified electrode based on nucleic acid oxidation, Electrochem. Commun. 9 (2007) 1474–1479.
[11] L. Zhenyu, Y. Weiqiang, Z. Guiyun, L. Qida, Q. Bin, C. Zongwei, C. Guonan, An ultrasensitive colorimeter assay strategy for p53 mutation assisted by nicking endonuclease signal amplification, Chem. Commun. 47 (2011) 9069–9071.
[12] X. Haitao, Z. Xingwang, Label-free electrochemiluminescence detection of specific-sequence DNA based on DNA probes capped ion nanochannels, Analyst 139 (2014) 1732–1739.
[13] W. Yang, R. Li, Q. Wang, Q. Wei, C. Fu, Z. Lin, G. Chen, A micro-pressure sensor-based analytic platform and its application in thrombin quantification, Anal. Methods 7 (2015) 7985–7988.
[14] J. Xu, Z.-S. Wu, W. Shen, H. Xu, H. Li, L. Jia, Cascade DNA nanomachine and exponential amplification biosensing, Biosens. Bioelectron. 73 (2015) 19–25.
[15] L. Yuan, W. Tu, J. Bao, Z. Dai, Versatile biosensing platform for DNA detection based on a DNAzyme and restriction-endonuclease-assisted recycling, Anal. Chem. 87 (2015) 686–692.
[16] L. Yang, Y. Tao, G. Yue, R. Li, B. Qiu, L. Guo, Z. Lin, H. Yang, Highly selective and sensitive electrochemiluminescence biosensor for p53 DNA sequence based on nicking endonuclease assisted target recycling and hyperbranched rolling circle amplification, Anal. Chem. 88 (2016) 5097–5103.

[17] Y. Jia, F. Sun, N. Na, J. Ouyang, Detection of p53 DNA using commercially available personal glucose meters based on rolling circle amplification coupled with nicking enzyme signal amplification, Anal. Chim. Acta 1060 (2019) 64–70.
[18] H. Li, Z. Wu, L. Qiu, J. Liu, C. Wang, G. Shen, R. Yu, Ultrasensitive label-free amplified colorimetric detection of p53 based on G-quadruplex MBzymes, Biosens. Bioelectron. 50 (2013) 180–185.
[19] X. Ma, Z. Wang, S. He, C. Chen, F. Luo, L. Guo, B. Qiu, Z. Lin, G. Chen, G. Hong, Development of an immunosensor based on the exothermic reaction between H2O and CaO using a common thermometer as readout, ACS Sens. 4 (2019) 2375–2380.
[20] G. Fu, S.T. Sanjay, M. Dou, X. Li, Nanoparticle-mediated photothermal effect enables a new method for quantitative biochemical analysis using a thermometer, Nanoscale 8 (2016) 5422–5427.
[21] G. Fu, S.T. Sanjay, W. Zhou, R.A. Brekken, R.A. Kirken, X. Li, Exploration of nanoparticle-mediated photothermal effect of TMB-H2O2 colorimetric system and its application in a visual quantitative photothermal immunoassay, Anal. Chem. 90 (2018) 5930–5937.
[22] X. Li, L. Yang, C. Men, Y.F. Xie, J.J. Liu, H.Y. Zou, Y.F. Li, L. Zhan, C.Z. Huang, Photothermal soft nanoballs developed by loading plasmonic Cu2- xSe nanocrystals into liposomes for photothermal immunoassay of aflatoxin B1, Anal. Chem. 7 (2019) 4444–4450.
[23] Y. Tao, F. Luo, L. Guo, B. Qiu, Z. Lin, Target-triggered aggregation of gold nanoparticles for photothermal quantitative detection of adenosine using a thermometer as readout, Anal. Chim. Acta 1110 (2020) 151–157.
[24] W. Zhou, K. Hu, S. Kwee, L. Tang, Z. Wang, J. Xia, X. Li, Gold nanoparticle aggregation-induced quantitative photothermal biosensing using a thermometer: a simple and universal biosensing platform, Anal. Chem. 92 (2020) 2739–2747.
[25] W. Li, L. Wang, W. Jiang, A catalytic assembled enzyme-free three-dimensional DNA walker and its sensing application, Chem. Commun. 53 (2017) 5527–5530.
[26] S.D. Mason, Y. Tang, Y. Li, X. Xie, F. Li, Emerging bioanalytical applications of DNA walkers, Trac. Trends Anal. Chem. 107 (2018) 212–221.
[27] H. Chai, J. Xu, J. Xu, S. Ding, Y. Tang, P. Miao, Star trigon structure-aided DNA walker for amplified electrochemical detection of DNA, Electrochem. Commun. 99 (2019) 51–55.
[28] Z. Chen, C. Wang, L. Hao, R. Gao, F. Li, S. Liu, Proximity recognition and polymerase-powered DNA walker for one-step and amplified electrochemical protein analysis, Biosens. Bioelectron. 128 (2019) 104–112.
[29] N. Li, M. Du, S. Tian, X. Ji, Z. He, The behavior of a bipedal DNA walker moving on the surface of magnet microparticles and its application in DNA detection, Anal. Bioanal. Chem. 411 (18) 4055-4061.
[30] F. Yang, X. Zhong, X. Jiang, Y. Zhuo, R. Yuan, S. Wei, An ultrasensitive aptasensor based on self-enhanced Au nanoclusters as highly efficient electrochemiluminescence indicator and multi-site landing DNA walker as signal amplification, Biosens. Bioelectron 130 (2019) 262–268.
[31] L. Wang, C.Y.J. Yang, C.D. Medley, S.A. Benner, W.H. Tan, Locked nucleic acid molecular beacons, J. Am. Chem. Soc. 127 (2005) 15664–15665.
[32] Y. Zhang, L. Wang, F. Luo, B. Qiu, L. Guo, Z. Weng, Z. Lin, G. Chen, An electrochemiluminescence biosensor for Kras mutations based on locked nucleic acid functionalized DNA walkers and hyperbranched rolling circle amplification, Chem. Commun. 53 (2017) 2910–2913.
[33] G. Frens, Controlled nucleation for the regulation of the particle size in monodisperse gold suspensions, Nat. Phys. Sci. (Lond.) 241 (1973) 20.
[34] Y. Huang, D.-H. Kim, Synthesis and self-assembly of highly monodispersed quasispherical gold nanoparticles, Langmuir 27 (2011) 13861–13867.
[35] S. Qiu, X. Li, W. Xiong, L. Xie, L. Guo, Z. Lin, B. Qiu, G. Chen, A novel fluorescent sensor for mutational p53 DNA sequence detection based on click chemistry, Biosens. Bioelectron. 41 (2013) 403–408.
[36] W.H. Zhao, H.B. Li, Y.Q. Tang, M.B. Liu, S.Q. Wang, R.Q. Yu, Fluorometric determination of the p53 cancer gene using strand displacement amplification on gold nanoparticles, Microchim. Acta 186 (2019) 517.
[37] D. Su, N. Li, Y. Liu, M. Wang, X. Su, Ratiometric fluorescence strategy for p53 gene assay by using nitrogen doped graphene quantum dots and berberine as fluorescence reporters, Anal. Chim. Acta 1084 (2019) 78–84.
[38] Y. Liu, X.Q. Chen, Q. Ma, A novel amplified electrochemiluminescence biosensor based on Au NPs@PDA@CuInZnS QDs nanocomposites for ultrasensitive detection of p53 gene, Biosens. Bioelectron. 117 (2018) 240–245.